AFCRL-63-467

ASTIA Document No. _____

Contract AF 61(052)-330 T(F) R

TECHNICAL (FINAL) REPORT

Research on the Synoptical Measurements of the Vertical Ozone Distribution

by

H. K. Paetzold

Institute of Geophysics and Meteorology

University Cologne

(Formerly Technische Hochschule Munich)

January 1, 1963

Prepared for

GEOPHYSICS RESEARCH DIRECTORATE

OFFICE OF AEROSPACE RESEARCH

AIR RESEARCH AND DEVELOPMENT COMMAND

UNITED STATES AIR FORCE

BEDFORD, MASSACHUSETTS

ASTIA DOCUMENT NO: _____

CONTRACT AF 61(052)-330 T(F)R

TECHNICAL (FINAL) REPORT

RESEARCH ON THE SYNOPTICAL MEASUREMENTS OF THE VERTICAL OZONE DISTRIBUTION

BY

H. K. Paetzold

Institute of Geophysics and Meteorology

University Cologne

January 1, 1963

The research reported in this document has been sponsored by Air Force Cambridge Research Laboratories of the AIR RESEARCH AND DEVELOPMENT COMMAND, UNITED STATES AIR FORCE, through its European Office.

TABLE OF CONTENTS

LIST OF FIGURES

Abstract:

This report continuous the Technical Report No. 1 from December 1, 1962. The evaluation procedure of the soundings with the optical ozone sonde is described in some further details. The meridional variations of the vertical ozone profile is derived from the soundings of the program. The correlation of the ozone variation with the weather situation is studied. At last, simultaneous ozone soundings and stratospheric warmings are presented.

I. Introduction:

In a first Technical Note from December 1961 [+)] the author has given a first short description of our optical ozone sonde and its evaluation procedure. This research program was outlined. Some ozone soundings of the international test program at Arosa in Summer 1961 have been demonstrated as an example.

Meanwhile the ozone soundings have been continued at Weissenau, Uccle (Institute of Prof. Van Mieghem) and Berlin (Institute of Prof. Scherhag). In total, about 200 sondes have been launched in Europe, America and India for this research program. The results combined with those of our IGY-Program give a first fine picture of the meridional cross section of the vertical ozone profile and the correlation between the ozone variations and the local weather conditions. A clear connection could be found between the jet streams and the vertical ozone profile between 10 and 20 km altitude. As a further extremely interesting result a narrow correlation between stratospheric ozone and the sudden stratospheric warmings could be discovered by direct balloon soundings. This correlation strongly supports the assumptions that the sudden stratospheric warmings in late winter and spring are caused by downwards motions of the stratospheric air.

[+)] Further named TN 1

From the combined analysis a worldwide ozone system could be derived. A strong photochemical ozone source must be concluded between 15 and 25 km altitude for the tropics and subtropics. From this region an ozone flux exists to higher latitudes predominantly in spring times, where it is pumped through the troposphere gaps into troposphere and the earth surface, where the worldwide ozone sink must be located.

Further new test flights were made by WMO in April 1962 in Arosa for ozone sondes of the optical and chemical types. In general, the agreement of our optical sonde with the chemical sondes of Brewer and Regener was satisfactory, though the ozone variations were pretty large in the lower stratosphere between 10 and 20 km in this season.

At last, the electronic computer program was further checked. Especially the convergency of the smoothing procedure of the sonde readings was proved.

In the following the smoothing procedure will be described in somewhat more detail. Then some examples will be given for the equatorial ozone profile. The correlation ozone and weather will be demonstrated for some examples. The derived meridional ozone correlation and its difference to the theoretical photochemical one will be discussed.

At last, the correlation between ozone variation and sudden stratospheric warmings will be demonstrated for January and February 1962

at Berlin. This phenomena must be regarded as the best link of the chain represented by ozone formation and destruction and the atmospheric air transport.

II. Electronic computing program:

The basic formula for the evaluation program can be written as:

$$(1)\quad x(h) = \frac{\log A - \log \frac{U(h,z)}{B(h,z)} - M(h,z)\,\Delta K_R + \log Sc(h,z)}{\alpha \cdot \sec z}\ cm O_3$$

$$(1a)\quad Sc\,(h,z) = \frac{U_{Sc}(h,z)}{B_{Sc}(h,z)}$$

with

$U(h,z)$: reading of the sonde in the UV-region +)

$B(h,z)$: reading of the sonde in the Blue-region

α : the effective spectral absorption coefficient of ozone (cm^{-1})

M : the effective air mass

ΔK_R : the difference of the rayleigh extinction for the UV- and the Blue-region

A : the relative spectral constant of the sonde

z : the solar zenith angle

+) For the spectral transmission of the filters in the UV- and Blue-region see TR 1, Sect.II.

h : the height

and x(h) : the vertical thickness of the ozone layer above the height h, which shall be determined.

The terms Sc(h,z) represents the sky light correlation since the quartz sphere receives a mixture of direct sunlight and scattered sky light. The terms $U_{Sc}(h,z)$ and $B_{Sc}(h,z)$ mean the intensity of the UV- and the Blue- scattered sky light.

As a sufficient good approximation we can set:

$$(2)\quad U_{Sc}(h,z) \approx \left[B_R(h,z) \left(\frac{\bar{\lambda}_\beta}{\bar{\lambda}_{UV}} \right)^4 + B_0(h,z) \left(\frac{\bar{\lambda}_\beta}{\bar{\lambda}_{UV}} \right)^{1,5} \right] \cdot 10^{-\alpha x(h) \sec z}$$

with

$$(2a)\quad B(h,z) = \int_{Bl} B_0(h) \cdot 10^{-M(h,z)\, K_R(h)} + B_R(h,z) + B_D(h,z)$$

$B_0(h)$ means the extraterrestrial spectral solar intensity.

The two terms in the brackets consider the rayleigh scattering and the dust scattering. Since the amount of the scattered sky

light rapidly decreases above two kilometers the simple separation of the two scattering processes only produces a negligible error.

It has been found from our ascents in Tromsö (North-Norway) that in polar regions the dust scattering is nearly zero so that the rayleigh function $B_R(h,z)$ in equation (2a) can be determined.

For tropical and subtropical stratospheric air masses beyond the tropopause gap the measured blue intensity $B(h,z)$ differs somewhat from the value found in polar regions. This difference must be caused by an additional dust scattering $B_D(h,z)$ in equ.(2) with a smaller dependence on wave length than the rayleigh scattering.

Fig. 1 shows the block diagram of the computer program developed for an IBM 650. It is devided into several subroutine to be sufficient flexible for some modification and improvements of the numerical function, which could be necessary according the experiences during the sounding program. The most important step is the smoothing of the measured $\log(U(h)/B(h))$ - curve. Since it was necessary the Blue-intensity and the Ultraviolet-intensity $U(h)$ to measure independently according equ. 1a, 2 and 2a, a certain scatter of the sonde readings is observed. The major reason is given by the fact that the intensity of light falling

from the quartz sphere on the photo cell varies within a few percent with the orientation of the sun to the axis of the quartz sphere [+)]. By this effect the swinging of the sonde causes a certain scatter of the single readings within $\pm$ 3 %.

For the determination of this random scattering we use a simple procedure (TN 1). For 16 readings the average is taken for a mean height $\overline{h_n}$ in the n^{th}-intervall of 0,7 km. Than the following simple formula is used three times:

$$(3) \quad \log \frac{U}{B}(\bar{h}_n) = \frac{1}{4} \log \frac{U}{B}(\bar{h}_{n-1}) + \frac{1}{2} \log \frac{U}{B}(\bar{h}_n) + \frac{1}{4} \log \frac{U}{B}(\bar{h}_{n-1})$$

By this we get the final used value $\overline{\overline{\log (U/B)}}$ (equ.8 in TN 1).

The mathematical meaning of this procedure is that the random statistical error $\Delta_{st} \overline{\overline{\log (U/B)}}$ is smaller than the difference $\Delta_{O_3}(U/B)$ corresponding in the average to an ozone thickness of $5 \cdot 10^{-4}$ cm O_3 NTP for the effective ozone absorption coefficient of the used UV-filter. The curve $\overline{\overline{\log (U,B)}}$ represents a polynom with about 40 independent coefficient for a sounding up to 30 km height.

As a proof for this procedure the curves $\log(U(h_n)/B(h_n))$, $\log\overline{(U/B)}$, $\log \overline{U/B}$ and $\log \overline{U/B}$ are plotted in Fig. 2 as an example[++)].

[+)] The ration U(h)/B(h) is nearly independent.

[++)] In Fig. 2 the functions log (U/B) a.s.o. are called Z_i for simplicity.

It can be well seen that the procedure quickly converges. The differences between the functions $\overline{U/B}$ and $\overline{U/B}$ are only small so that the details of the last curve must be regarded as real and significant. This is also demonstrated by the measured ozone profiles at consecutive days or at neighboured launching places with the same weather conditions as it can be seen in Fig. 6.

In these cases the derived details are similar or vary only slowly as it must be expected if the evaluation procedure is correct.

III. The equatorial vertical ozone profile:

It is well known that for low latitudes the smallest total thickness of the ozone layer is observed contrary to the photochemical theory. While at the equator a value of 0,2 cm O_3 NTP is found (1). From the indirect Umkehr-measurements (Götz-Effect) it has been further found that the mean height of the ozone layer is considerable greater in lower latitudes.

In our IGY-program 1957/58 the polar and equatorial vertical profiles have been determined for the first time by direct balloon soundings at the stations Leopoldville/Congo (5° S) and Tromsö/ Norway (70° N)(1a). Two typical examples have been given in Fig. 1 of TN 1. In Fig. 3 two further ozone profiles at Leopoldville are demonstrated.

It was of extreme interest to prove whether this typical shape found over central Africa is representative for the whole tropical zone or not. Therefore, for this program flights with the optical ozone sonde were made at Albrook/Canal Zone and Hyderabad/India +). In Fig. 4 vertical ozone distributions are given at these two stations. It can be well seen that these profiles are extremely similar to those measured at Leopoldville. It is important that Leopoldville and Albrook are located in a quite different geographical situation. Leopoldville is surrounded by large land masses while Albrook lies between two great oceans. It must be expected that the ozone destruction in the lower troposphere and at the earth surface will somewhat differ for oceans and continents. From the similarity of the stratospheric ozone profiles in Leopoldville and Albrook it must be concluded that these differences above are only of minor influence for the higher ozone. Combined with the Indian ascents we can define an "equatorial ozone type" with the following features:

a) The main part (90 %) of the ozone layer is located above 18 to 20 km. Below this altitude the ozone content does not exceed 1 Dobson-Unit (10^{-3}cm O_3/km). It is remarkable that the ozone increases not exactly at the height of the tropical tropopause but in general 3 km above.

+) The Indian flights were possible by the great help of Dr. Junge/Air Research and Prof. Ramanathan.

b) The ozone profile is sharp. The absolute ozone maximum is located at 27 to 28 km height.

c) Nearly no seasonal variations exist

A contrary ozone profile we have found at Tromsö (70° N) by our IGY ozone soundings (Fig. 1, TN 1). This polar profile can be characterized as follows:

a) In the yearly average 40 % of the ozone layer is found below 20 km height (60 % in spring, 20 % in late autumn).

b) The ozone profile is generally broad, since the increase of ozone starts already at an altitude of about 10 km. The absolute ozone maximum is found at about 22 km height. The ozone increase starts just above the tropopause.

c) A strong seasonal variation exists for the polar ozone profile. The ozone amount below 20 km has its maximum in spring time and decreases towards autumn. This variation of the lower polar ozone mainly causes the long known seasonal variation of the total ozone amount in height and middle latitudes.

IV. Ozone variations and weather conditions:

It is known for a long time that the total ozone amount shows a strong correlation to the weather activity in mean and high

latitudes. In general, a maximum is found in low pressure troughs and a minimum in high pressure ridges (2). A strong negativ correlation exists between the height of the tropopause and the total ozone amount (3)(4). Balloon born ozone sondes give the possibility to solve the problem in which region of height these ozone variations are mostly concentrated. In the following some examples of our ozone soundings at Weissenau, Uccle and Arosa are discussed. The general problem is that the variations of the vertical ozone profile are caused by horizontal and vertical air transport. To distinguish between these two processes for one given place a whole net of ozone sounding stations is necessary. But the principle features can be seen already from the given examples.

a) Ascents at Weissenau ($9^{o}35^{m}$E) and Uccle ($4^{o}22^{m}$ E):

Both launching places are located at a distance of about 520 km from each other. The soundings were made at the same day at nearly the same hour.

In Fig. 5 two ascents are given for Weissenau alone. The weather situation is characterized by the isobares at the 200 mb level. At the two launching days the weather situation was quite contrary. At the 18th April a strong trough crossed South Germany. The jet stream zones were southwards of Weissenau. A strong secondary maximum of low stratospheric ozone was observed, which was the

main cause for the considerable ozone increase at this day. At the 21st April a high pressure ridge up to 15 km height had reached Weissenau. The amount of the ozone between 10 and 20 km was found low reducing the total ozone amount.

The shape of the secondary maximum varies strongly as other flights have shown. Sometimes it is well pronounced and sharply separated from the primary photochemical maximum above 20 km height. At other days the secondary ozone maximum is flat and nearly not separated from the primary maximum. The same features are shown by Figures 6 and 7 demonstrating some simultaneous ascents at Uccle and Weissenau. Again the secondary ozone maximum is connected with a trough situation. The secondary low stratospheric ozone maximum is strongest for the station, which is deeper located in the trough. The example of the 11th and 13th August is very instructive. At the 11th August Uccle is located just within the eastern edge of a trough, while Weissenau is just outwards of it. The secondary ozone maximum at Uccle is much more pronounced as at Weissenau. At the 13th August the trough has somewhat swept westwards so that the location of Uccle in the trough-ridge system is similar to that of Weissenau at the 11th. Consequently the ozone profile at Uccle at the 13th has been found the same as that at Weissenau two days before the 11th August. It must be taken attention to the extreme similarity of the final details of the ozone profiles at Weissenau for the 11th

and at Uccle for the 13th August.

This narrow connection between the secondary ozone maximum and the subtropic jet has been also found by us at other places, e.g. at Denver during the ozone sonde test flights in April 1959 (5). Due to the fact that over the large northamerican continent the trough-ridge system is more pronounced and their movements are much more regular the variations of the low stratospheric ozone are much more pronounced and impressive.

Finally we have found from other ascents that sometimes a tertiary tropospheric ozone maximum at 6 km height is observed, which is weaker than the secondary maximum above. It mostly occurs if a pronounced polar jet stream passes. Probably this tertiary ozone maximum must be correlated to the temporary break between the mean latitude and the high latitude tropopause.

b) <u>The Arosa test flights April 1962:</u>

Since the relative concentrations of the atmospheric ozone don't exceed a value of 5 ppm it is of greatest importance to measure the vertical ozone profile by different total independent methods to avoid systematical errors. Therefore the comparision of our optical sonde with the chemical sondes of Brewer and Regener at Arosa 1961 and 1962 were of great value. Our soundings at Arosa in summer 1961 have been already published in the preceding

TN 1. The Figures 8 - 13 give our soundings of the test in April 1962. At both test programs the results of the different types of ozone sondes have been found in general agreement. The observed minor differences do not influence the general conclusions.

In August 1961 the weather situation did not change strongly. Mostly Arosa was situated northwards of the jet stream belt during the launching days. Only at the 30.7.1961 Arosa was located right at the edge of a trough. Consequently a considerable amount of ozone was found between 10 and 20 km according Fig. 11 in TN 1. Further in this season the low polar stratospheric ozone has already markedly decreased.

Contrary, in April 1962 several pronounced troughs passed Arosa, while the polar reservoir of deep ozone was not yet exhausted. In excellent agreement with our own previous results above the optical Paetzold-sonde, the wet chemical Brewer-sonde and the dry chemical Regener-sonde give the same result: namely the existence of a secondary ozone maximum between 10 and 20 km, which sharpness varied. This secondary ozone maximum generally starts at the height of the tropopause.

In Fig. 14 the weather situations are demonstrated for the Arosa ascents 1962 again for the 200 mb level. The ozone variations are again narrow correlated to the location of the jet stream (thick arrows). Take attention e.g. to the strong decrease of the

ozone above 10 km height when the jet stream zone swept over Arosa from West to East from the 11th to the 12th April.

Besides this effect of advection also the influence of vertical air motions can be seen by comparing ozone distributions in a trough but eastwards and westwards of its axis (e.g. 11th and 16th April 1962). From the figures 8 - 13 it can be well seen that the amount of the secondary ozone maximum is generally great if its altitude is lower, so that the ratio of O_3/Air remains nearly constant. This suggests that the amount of the secondary maximum strongly varied by vertical air movements. Since in this region the relative ozone concentration strongly increases with altitude the absolute ozone content (the number of O_3 - molecules/cm^3) must be enlarged by downwards air movements and vice versa according the equation:

$$(4) \qquad \frac{d[O_3]}{dt} = -V_K \left(\frac{d[O_3]}{dh} - \frac{1}{\rho} \frac{d\rho}{dh} [O_3] \right)$$

$[O_3]$: Numbers of $[O_3]$ -molecules/cm^3

ρ : Air density

V_K : Vertical velocity of air

From the variation of the vertical ozone air movements within $\pm$ 2 km must be concluded between 10 and 20 km. The strongest and

deepest secondary O_3 - maximum is observed in the western part of a trough (e.g. 7th and 11th April 1962) as it also has been found by other ozone ascents. This is in excellent agreement with the fact that the highest values of the total ozone amount are observed westwards of the center of a cyclon in Palmen's tropopause funnel. On the other hand, the secondary ozone maximum is located at higher altitudes and its absolute value is smaller (16th and 19th April 1962). So we have to conclude a downwards motion from the eastern to the western part of a trough.

c) General conclusions:

From our own ozone soundings at different places and different seasons represented by the examples above the following conclusions can be drawn for the correlation between vertical ozone profile and weather:

1. In middle latitutes the ozone profile changes between the equatorial and the polar type.

2. The distinct boundary between the equatorial and the polar ozone type is formed by the zone of the break between tropical and the mean latitude tropopause.

3. The major part of the interdiurnal ozone variation in mean latitudes is caused by the ozone fluctuation in the lower stratosphere between 10 and 20 km (secondary ozone maximum).

4. These fluctuations are caused by advection of stratospheric, polar or subtropical air masses and by vertical air motions. In spring times the role of advection is stronger than that of the vertical motion (by about the factor 2) and vice versa for the autumn.

V. Meridional ozone cross section and world-wide ozone transport:

Since our soundings with our optical sonde (about 400) have been taken at a world-wide scale and in different seasons it is possible to derive a first meridional ozone cross section based on direct balloon measurements. In Fig. 15 the meridional ozone distribution is given for spring and autumn as the season for which the differences are most pronounced. The dotted and the full curves give the lines of constant absolute ozone content in Dobson-units (10^{-3} $cm O_3/km$), while the pointed curves represent the ozone distribution according the photochemical theory alone. The ozone values were calculated for the photochemical equilibrium with the formulas (6):

(5)

$$O_2 + h\nu \rightarrow O + O$$

$$O_3 + h\nu \rightarrow O + O_2$$

$$O + O_2 + M \rightarrow O_3 + M \qquad K_1 \text{ Kinetic factor}$$

$$O_3 + O \rightarrow O_2 + O_2 \qquad K_2 \text{ Kinetic factor}$$

The ozone concentration $[O_3]$ in O_3-mol/cm^3 results to:

$$(6)\quad [O_3](h,z) = C_{O_2} \sqrt{[M(h)]^3} \sqrt{\frac{K_1}{K_2} \frac{i_{1,abs}(h,z)}{i_{2,abs}(h,z)}}$$

with

$$(6a)\quad i_{1,abs}(h,z) = 2{,}3 \int J(\lambda,h,z) \cdot \alpha_{O_2}(\lambda)\, d\lambda$$

$$i_{2,abs}(h,z) = 2{,}3 \int J(\lambda,h,z) \cdot \alpha_{O_3}(\lambda)\, d\lambda$$

The ozone concentration $\varepsilon(h)$ in Dobson units cm O_3/km is given by

$$(6b)\quad \varepsilon(h) = \frac{[O_3](h)}{N_A} \cdot 10^{-5}$$

It means

$\alpha_{O_2}(\lambda)$	:	the spectral absorption coefficient of oxygen
$\alpha_{O_3}(\lambda)$	:	the spectral absorption coefficient of oxygen for O_3
$[M](h)$	:	the particle density for air at the height h
z	:	zenith angle of the sun
$J(\lambda,h,z)$	:	the solar spectral intensity at the height h, the zenith angle z, and the wave length λ
N_A	:	Avogadro's number

For the calculation the best new values for the solar UV-emission and the reaction coefficient were used. In formula 6 and 7 the recombination of atomic oxygen to molecular oxygen has been neglected, which is valid up to an altitude of 50 km.

From Fig. 15 it can be well seen that within the belt of the subtropical stream and up to an altitude of 20 km the ozone concentration is very small. In theselatitudes the observed ozone concentration is smaller than that following from the photochemical equilibrium between 10 and 25 km height. Therefore in this region ozone must be photochemically formed according the equations:

$$(7)\quad \frac{d[O_3]}{dt} = K_1 [O_2][O][M] - K_2 [O_3][O] - J_{abs,O_3}$$

$$\frac{d[O_2]}{dt} = J_{abs,O_3} + 2\, J_{abs,O_2} - K_1 [O_3][O][M] - K_2 [O][O_3]$$

with

$$(7a)\quad J_{abs,O_2} = 2{,}3\, c_{O_2} \cdot \frac{[M]}{N_A} \int J(\lambda,h,z)\alpha_{O_2}\, d\lambda$$

$$J_{abs,O_3} = 2{,}3\, \frac{[O_3]}{N_A} \int J(\lambda,h,z)\, \alpha_{O_3}\, d\lambda$$

For this photochemical ozone reproduction an average strength of $1 \cdot 10^{11}$ O_3 mol/cm^2 cln/sec follows for the low latitude stratospheric photochemical ozone source.

Beyond the subtropical tropopause break the measured ozone content is considerable greater than the photochemical values for all altitudes below 25 km. This fact strongly imposesan atmospheric transport system by which this low stratospheric ozone must be accumulated in higher latitudes. Further the local photochemical ozone formation above 25 km seems to be too weak by the factor 5 to 10 in these higher latitudes to produce this accumulation (especially the spring time increase) and to balance the ozone sink in the lower troposphere and at the ground with a strength of also $1 \cdot 10^{11}$- mol/cm^2 coln/sec, which magnitude is in agreement with other authors (7) +).

Therefore we have assumed a meridional O_3 - transport from the low latitude photochemical ozone source up to higher latitudes, where it is brought down in the lower stratosphere. The intensity of this world-wide transport mechanism is most intensive in late winter and early spring and causes the seasonal increase of ozone in this season for middle and high latitudes. (See the following section VI.). Whether the meridional transport is represented by

---

+) A tropospheric secondary O_3 - source of this strength by electrical discharge is probably weaker by the factor 100.

a direct slow circulation according the Brewer model or by a large eddy-exchange mechanism cannot be decided. In the polar and subtropical tropopause breaks the low stratospheric ozone is pumped into the troposphere, where it is fast brought down by vertical turbulance to the earth surface as the major ozone sink.

According our observations of the ozone variations the jet stream must be regarded as that zone, where the major part of the exchange between the troposphere and the stratosphere takes place. The mean time scale for a transport from the low latitude stratosphere to the middle and the high latitude troposphere results about two years in agreement with observations of the radioactive fall out.

VI. Stratospheric warmings and vertical ozone profile:

In Fig. 15 it is demonstrated that a considerable ozone amount is accumulated below 20 km height beyond the jet stream belt. It has been further pointed out that this low polar ozone cannot be photochemically formed in this region. On the other hand it is well known that in late winter and early spring sometimes the stratospheric temperatures suddenly rise, which has been first observed by Scherhag in Berlin 1952 (8). These stratospheric warmings have been observed now every year. They seem mostly to occur over the North Canadian area. Since the necessary energy amount for the warmings is far too large to be explained by extraterrestrial

variable sources (solar UV- or corpuscle invasions) only the assumption seems to be reasonable that the warmings are caused by adiabatic heating due to downwards motions of the air. So this warmings seem to be the consequence of the step-by-step break down of the winterly stratospheric circupolar vortex, which is caused itself by the strong meridional temperature gradient on the winter hemisphere in the warm layer due to the ozone absorption of solar UV-radiation.

The assumption, whether the sudden stratospheric warmings are caused by subsidences can be proved by the vertical ozone profile itself. According equation (4) downwards motions will increase the absolute ozone content if the ratio $\left[O_3\right]/\rho$ increases with height. This is surely the case for the atmospheric ozone layer up to an altitude of about 30 to 35 km. Consequently the absolute amount of the main part of the ozone layer will be enlarged by a downwards air circulation and vice versa.

In the year 1962 special ozone flights were made at Berlin to determine the vertical ozone distribution during stratospheric warmings. The result is represented in Fig. 16 and 17 on the new "Godson-Ozonagram"-paper. On the left side the ozone profiles are given, while the simultaneously measured stratospheric temperatures are shown on the right side of the diagrams.

A clear correlation can be drawn from the ascents in Fig. 16 and 17

warm stratosphere $\leftrightarrow$ high ozone value

cold stratosphere $\leftrightarrow$ low ozone value

E.g. at the 18th January 1962 the lowest stratospheric temperatures of $-80^{\circ}C$ were measured, which were ever observed over Berlin. The corresponding ozone values are extremely small. Contrary twice more ozone was observed at the 20th February 1962, when the stratospheric temperatures were gone up to $-40^{\circ}C$. These results of our direct soundings are in well agreement with recent observations of the enlargement of the total ozone amount during stratospheric warmings (9)(10). From the curves in Fig. 16 and 17 we have to conclude that the major part of the total ozone is located in the heights between 10 and 25 km.

From the meridional cross section (Fig. 15) follows that in no regions in general ozone concentrations of 25 Dobson-units ($10^{-3} cm O_3/km$) are representative, which corresponds to the maximum ozone value in Fig. 17. Therefore this high ozone concentration must be produced by subsidence of air at one place, from where it will be transported to other regions by advection.

It is of interest to compare the vertical air displacements, which are necessary to produce the observed ozone and temperature variat-

ion in Fig. 16 and 17. For the latter a vertical dry-adiabatic lapse rate of -10^{o}/km was assumed. Let be Δh_{O_3} the displacement for the ozone variation according equ.(4) and Δh_T that for the temperature variations than we get from the curves the following mean relationship:

$$(8) \qquad \Delta h_T = 0{,}75 \ (\pm 0{,}1) \cdot \Delta h_{O_3}$$

The general agreement is sufficient between Δh_{O_3} and Δh_T to strengthen the assumption that the stratospheric warmings are mainly caused by vertical motions. But according equ. (8) the observed temperature variations are only 75 % of that, which would follow from a pure adiabatic process. The most reasonable explanation is, that a temperature decrease has taken place by radiative cooling since the initial adiabatic heating took place. One can estimate that the heating of the observed air masses in Fig. 16 and 17 occured about one week before the observations were taken over Berlin. Apparently the ozone is a considerable more conservative parameter for the dynamics of the atmosphere than the temperature below a height of about 30 km.

Only little doubt can be anymore that the yearly replenishment of the low polar ozone in late winter and early spring is mainly caused by the vertical subsidence connected with the break down

of the winterly stratospheric circulation.

These first direct ozone observations above during stratospheric warmings represent the last link in the chain of conclusions drawn from the meridional, seasonal and synoptical ozone variations in Section IVa and V. The typical meridional ozone profile in spring in Fig. 15 is restored every year by a world-wide circulation process, which is predominantly caused by the ozone layer itself.

VII. Summary:

The results above presents a conclusive picture of the large and small scale variation of the vertical ozone profile. As one main result the distinct boundary between the equatorial and polar ozone type must be pointed out as it is given by the jet stream zone. The different effects of advection and vertical air motions can be clearly distinguished by the ascents of our little net.

The clear correlation between ozone variations and stratospheric warmings demonstrates the significance of the ozone for the study of world-wide air circulations. On the other hand the ozone has been proved to be a much better parameter for different air masses than the temperature up to an altitude of 30 km. For the future it can be expected that a world-wide net of ozone soundings will

give important new information for the dynamics of the troposphere and the lower and middle stratosphere.

VIII. Acknowledgements:

First the author has to express his hearty thanks for the help of launching the ozone sondes at different stations, which was given by the Geophysical Research Directorate Bedford, Mass., the Meteorological Institute at Uccle, Prof. Van Mieghem, the Institute of Meteorology at West-Berlin, Prof. Scherhag. Further the assistance of my collaborators Dipl.Ing. F. Piscalar, Dipl.Phys. H. Zschörner and of Dipl.Met. E. Mädlow (Institute of Meteorology at Berlin) has strongly to be pointed. At last the program would not have been possible without the generous financial support of the Geophysical Research Directorate Bedford.

References

(1) H.K. Paetzold, "Ozon in der Erdatmosphäre" Encyclopedy of Physics, Vol. XLVIII Berlin,Heidelberg (1957)

(1a) H. K. Paetzold, a. F. Piscalar, Ber. Dt. Wetterdienst, 51, 128 (1959)

(2) G.M.B. Dobson, Proc.Roy. Soc.,London 129, 411 (1930)

(3) A.R.Meethan, Quart.J.Roy.Meteor.Sc. London, 63, 289 (1937)

(4) Chr.Normand, Quart.J.Roy.Meteor.Sc. London, 79, 39 (1953)

(5) H.K.Paetzold a.F.Piscalar, Naturw. 48, 474 (1961)

(6) H.K.Paetzold, Geof.Pur.e.Appl. 24, (1953)

(7) Chr. Junge, Proc.Int.Ozone Symp.Arosa 1961

(8) R.Scherhag, Ber.Dt.Wetterd. US-Zone, Nr.38 (1952)

(9) L. Godson, Proc.Int.Ozone Symp. Arosa 1961

(10) H.U.Duetsch, Beitr.Phys.d.Atmosph. 35, 87 (1962)

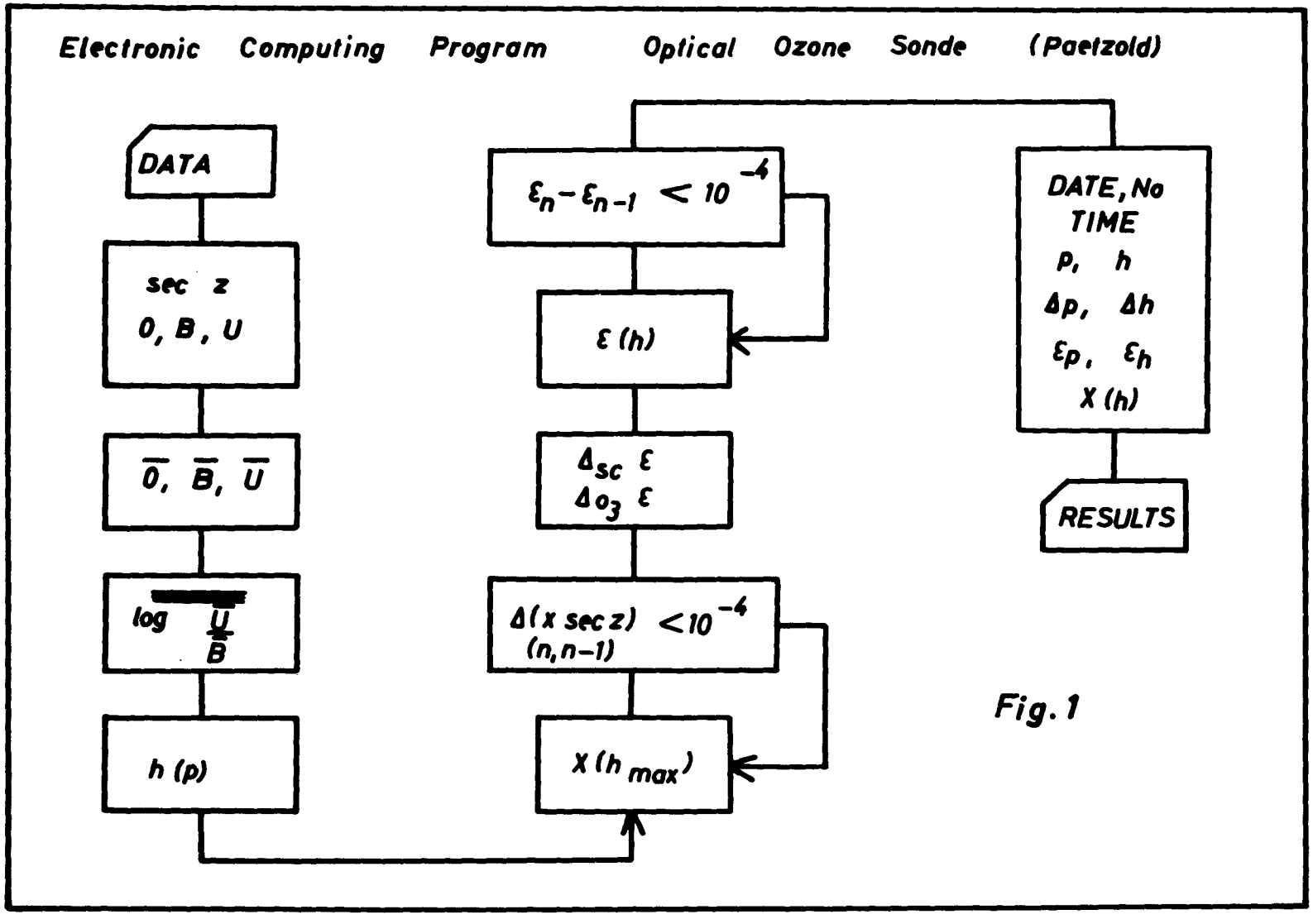
Electronic Computing Program Optical Ozone Sonde (Paetzold)
DATA
sec z
0, B, U
$\overline{0}$, $\overline{B}$, $\overline{U}$
log $\frac{\overline{U}}{\overline{B}}$
h (p)
$\varepsilon_n - \varepsilon_{n-1} < 10^{-4}$
ε (h)
Δ_{sc} ε
Δ_{o_3} ε
$\Delta(x \sec z)_{(n,n-1)} < 10^{-4}$
X (h_{max})
DATE, No
TIME
p, h
Δp, Δh
ε_p, ε_h
X (h)
RESULTS

Fig. 1

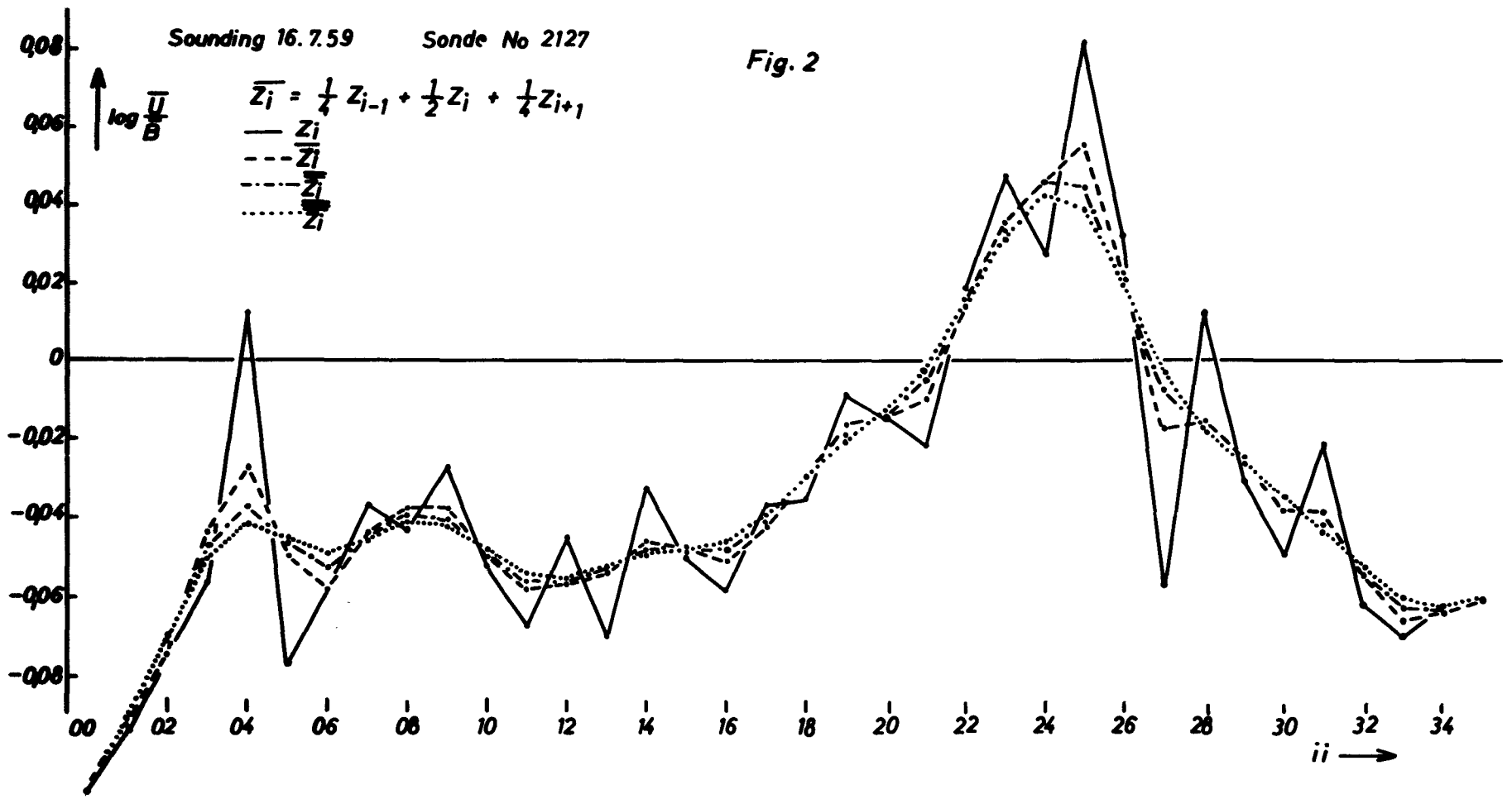
Sounding 16.7.59
Sonde No 2127
$\overline{z_i} = \frac{1}{4} z_{i-1} + \frac{1}{2} z_i + \frac{1}{4} z_{i+1}$
$\log \frac{U}{B}$
z_i
$\overline{z_i}$
$\overline{\overline{z_i}}$
$\overline{\overline{\overline{z_i}}}$
0,08
0,06
0,04
0,02
0
-0,02
-0,04
-0,06
-0,08
00
02
04
06
08
10
12
14
16
18
20
22
24
26
28
30
32
34
ii

Fig. 2

Fig. 3

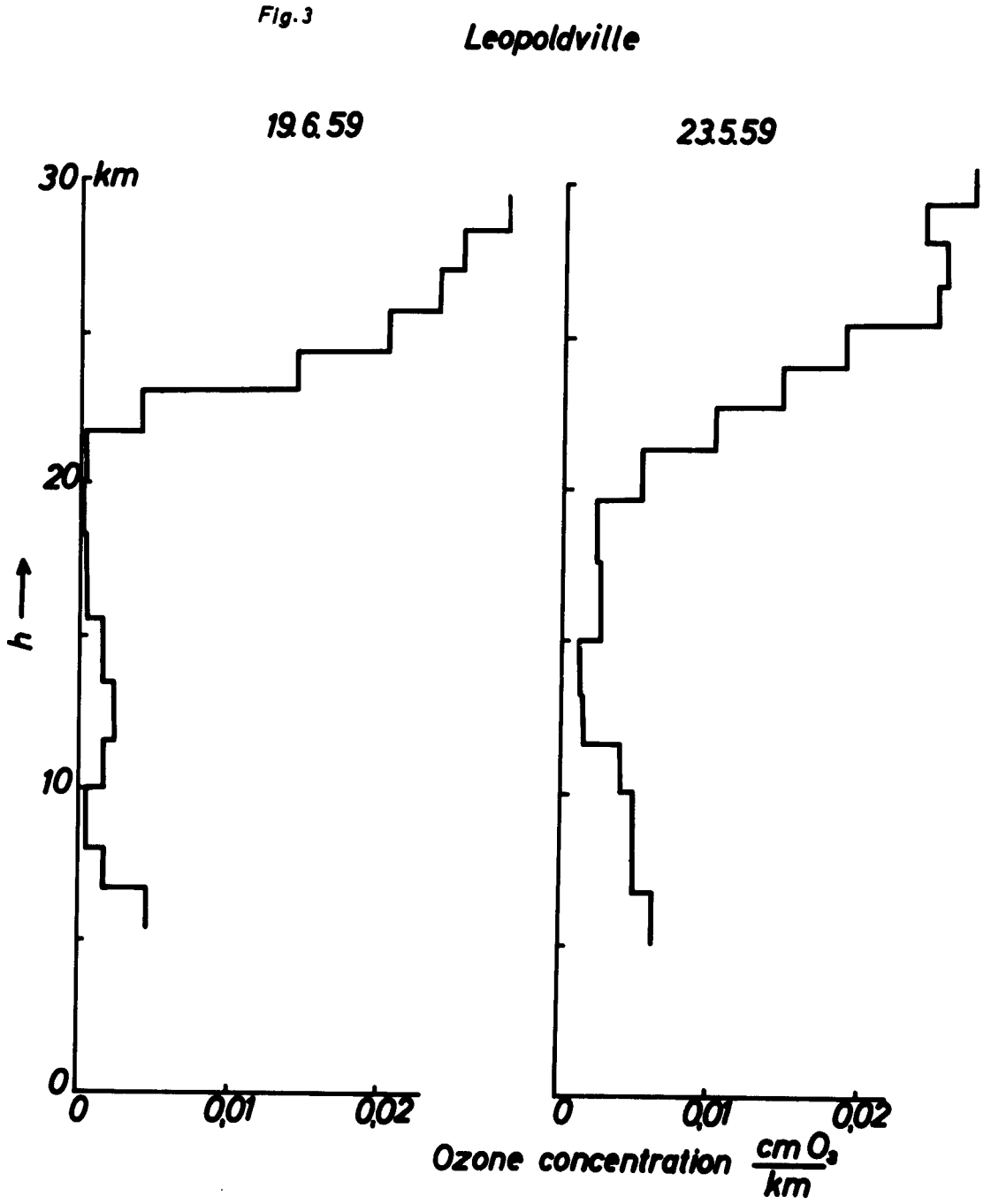
Leopoldville
19.6.59
23.5.59
30 km
20
10
0
h
0
0,01
0,02
0
0,01
0,02
Ozone concentration cm O3 / km

Fig. 4

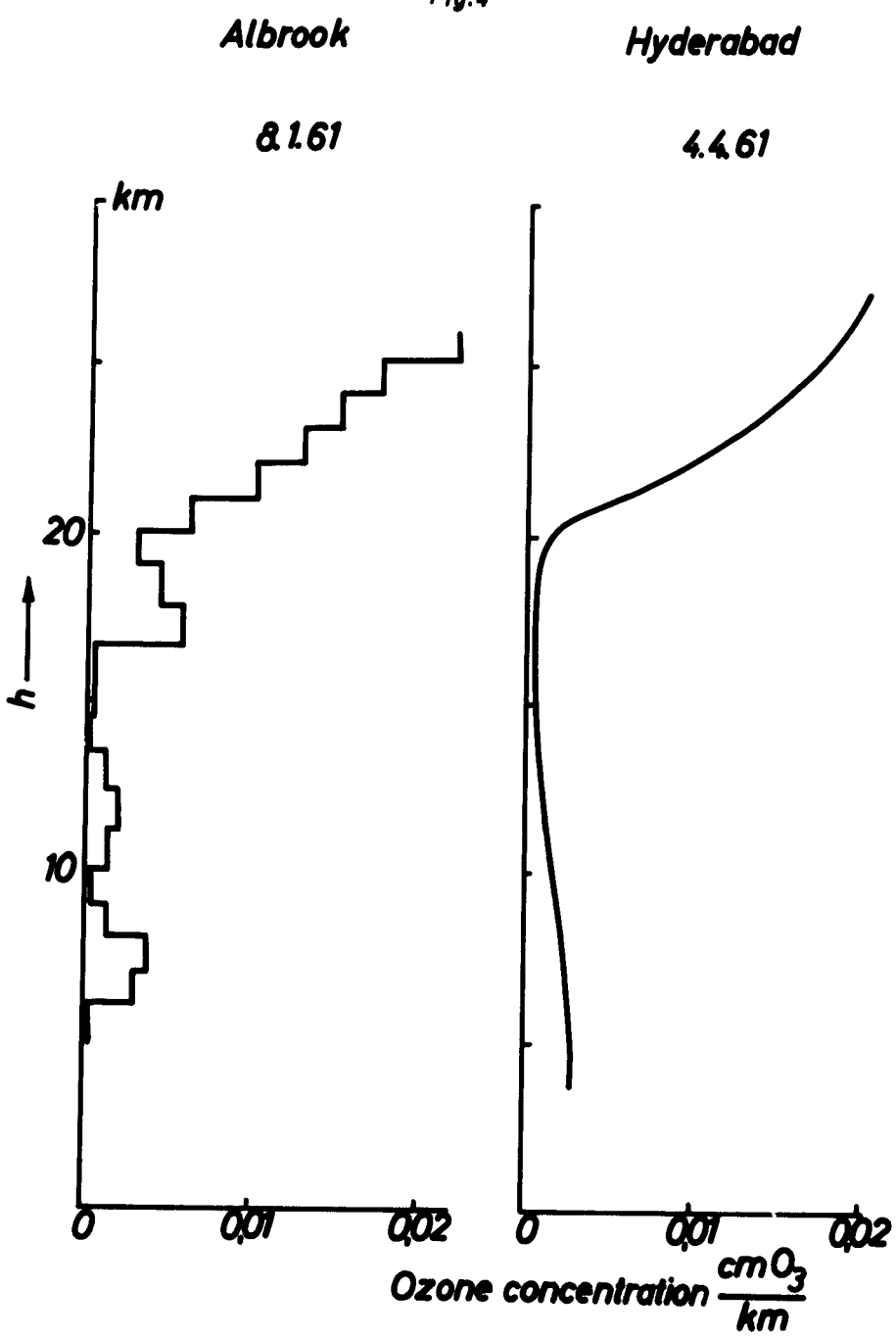
Albrook
8.1.61
Hyderabad
4.4.61
km
20
10
h
0
0,01
0,02
0
0,01
0,02
Ozone concentration $\frac{cm\,O_3}{km}$

Weissenau

Fig. 5

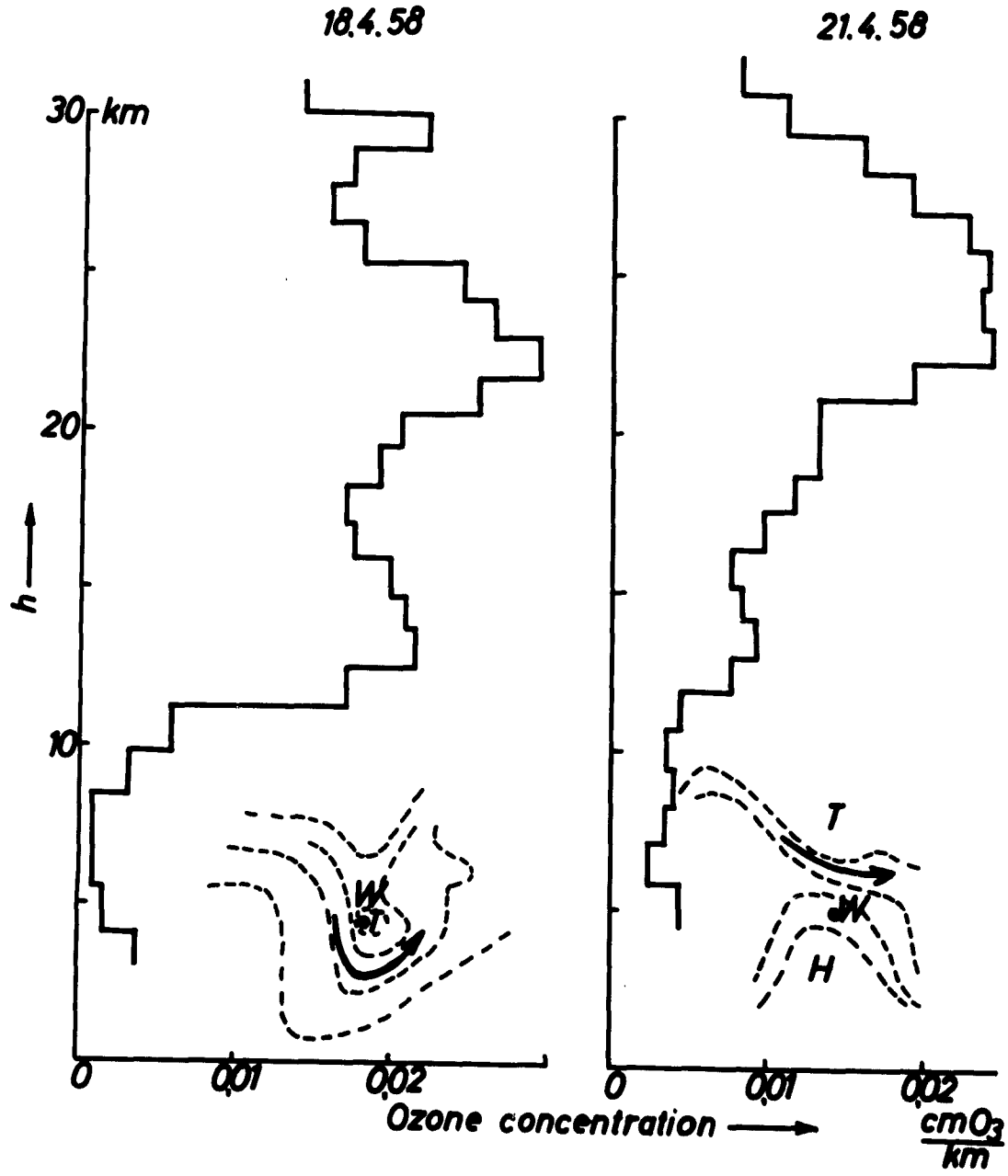

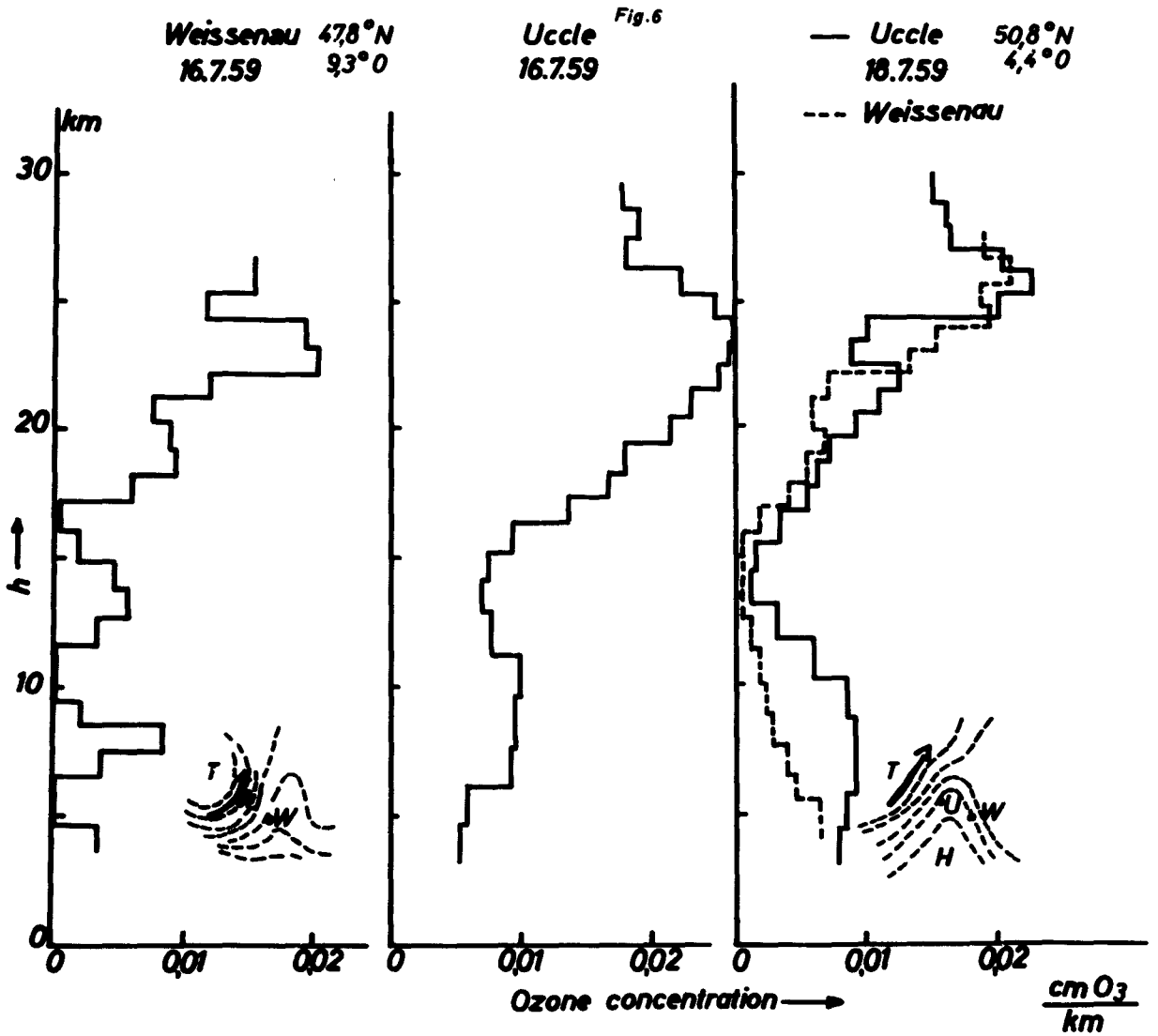
Weissenau 47,8°N
16.7.59 9,3°O
Uccle
16.7.59
Fig.6
— Uccle 50,8°N
18.7.59 4,4°O
--- Weissenau
km
30
20
10
0
h
0
0,01
0,02
T
W
H
Ozone concentration
cm O3
km

Fig.7

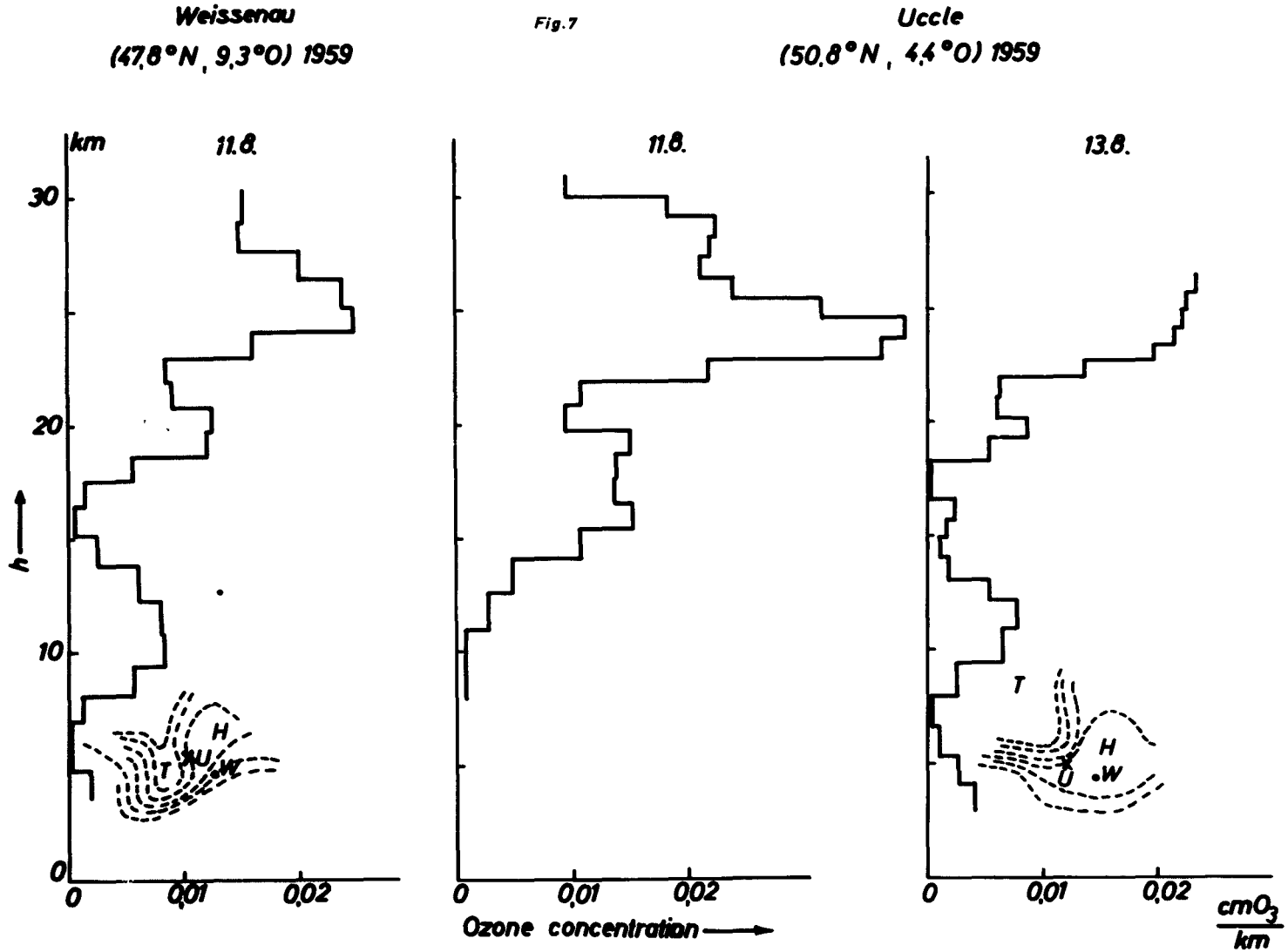
Weissenau
(47,8°N, 9,3°O) 1959
Uccle
(50,8°N, 4,4°O) 1959
km
11.8.
11.8.
13.8.
30
20
10
0
h
H
T
U
W
T
H
O
W
0
0,01
0,02
0
0,01
0,02
0
0,01
0,02
Ozone concentration
cmO3
km

OZONAGRAM

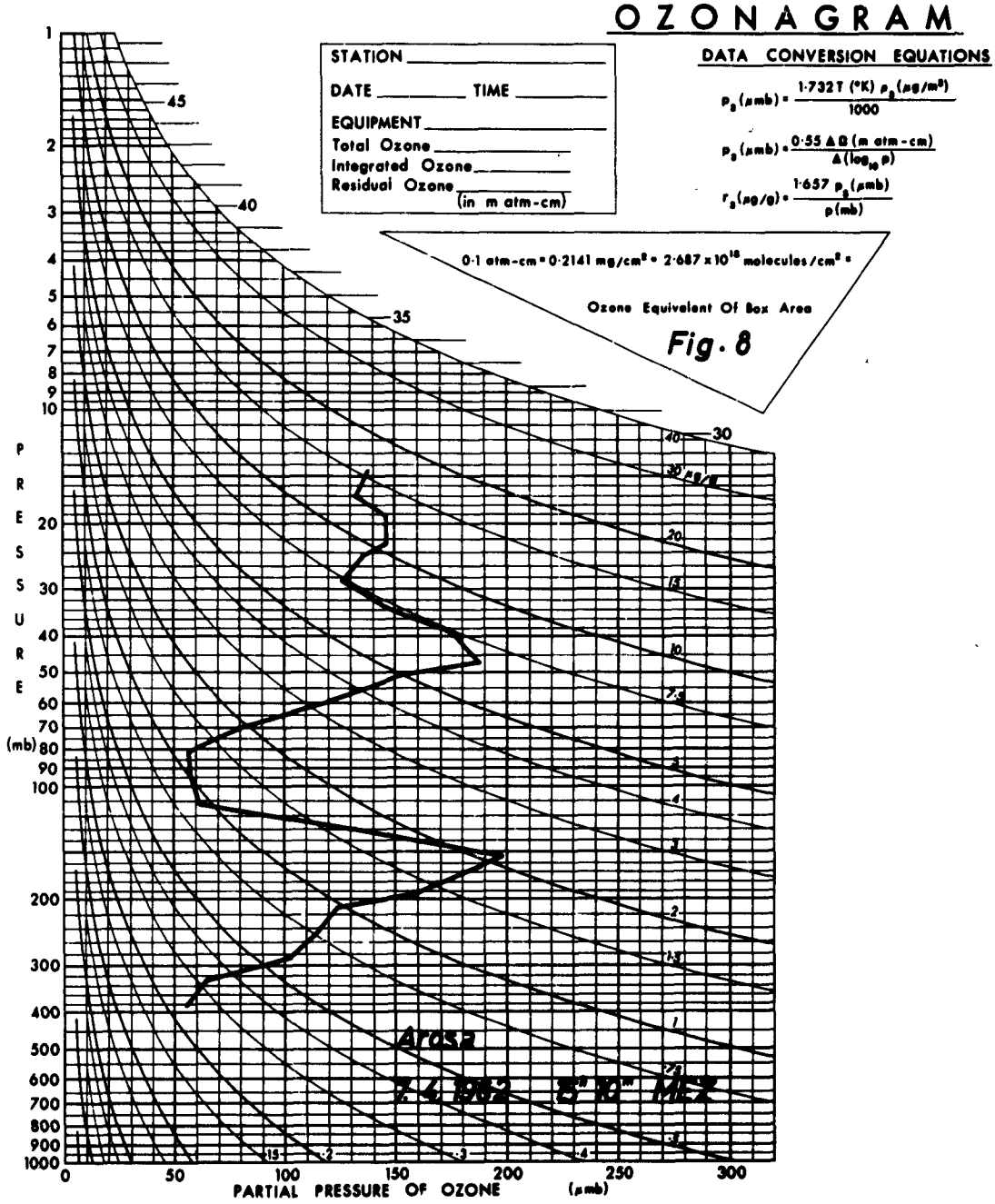
STATION
DATE TIME
EQUIPMENT
Total Ozone
Integrated Ozone
Residual Ozone
(in m atm-cm)
DATA CONVERSION EQUATIONS
$p_s(\mu mb) = \frac{1{\cdot}732\,T\,(°K)\,\rho_s(\mu g/m^3)}{1000}$
$p_s(\mu mb) = \frac{0{\cdot}55\,\Delta\Omega\,(m\ atm\text{-}cm)}{\Delta(\log_{10} p)}$
$r_s(\mu g/g) = \frac{1{\cdot}657\,p_s(\mu mb)}{p(mb)}$
0·1 atm-cm = 0·2141 mg/cm² = 2·687 x 10¹⁸ molecules/cm² =
Ozone Equivalent Of Box Area
Fig. 8
PRESSURE (mb)
PARTIAL PRESSURE OF OZONE (μmb)
1
2
3
4
5
6
7
8
9
10
20
30
40
50
60
70
80
90
100
200
300
400
500
600
700
800
900
1000
0
50
100
150
200
250
300
45
40
35
30
Arosa

OZONAGRAM

STATION _____

DATE _____ TIME _____

EQUIPMENT _____

Total Ozone _____

Integrated Ozone _____

Residual Ozone _____ (in m atm-cm)

DATA CONVERSION EQUATIONS

$$p_s(\mu mb) = \frac{1{\cdot}732\,T\,(^\circ K)\,\rho_s(\mu g/m^3)}{1000}$$

$$p_s(\mu mb) = \frac{0{\cdot}55\,\Delta\Omega\,(m\ atm\text{-}cm)}{\Delta(\log_{10} p)}$$

$$r_s(\mu g/g) = \frac{1{\cdot}657\,p_s(\mu mb)}{p(mb)}$$

0·1 atm-cm = 0·2141 mg/cm² = 2·687 x 10^{18} molecules/cm² =

Ozone Equivalent Of Box Area

Fig. 9

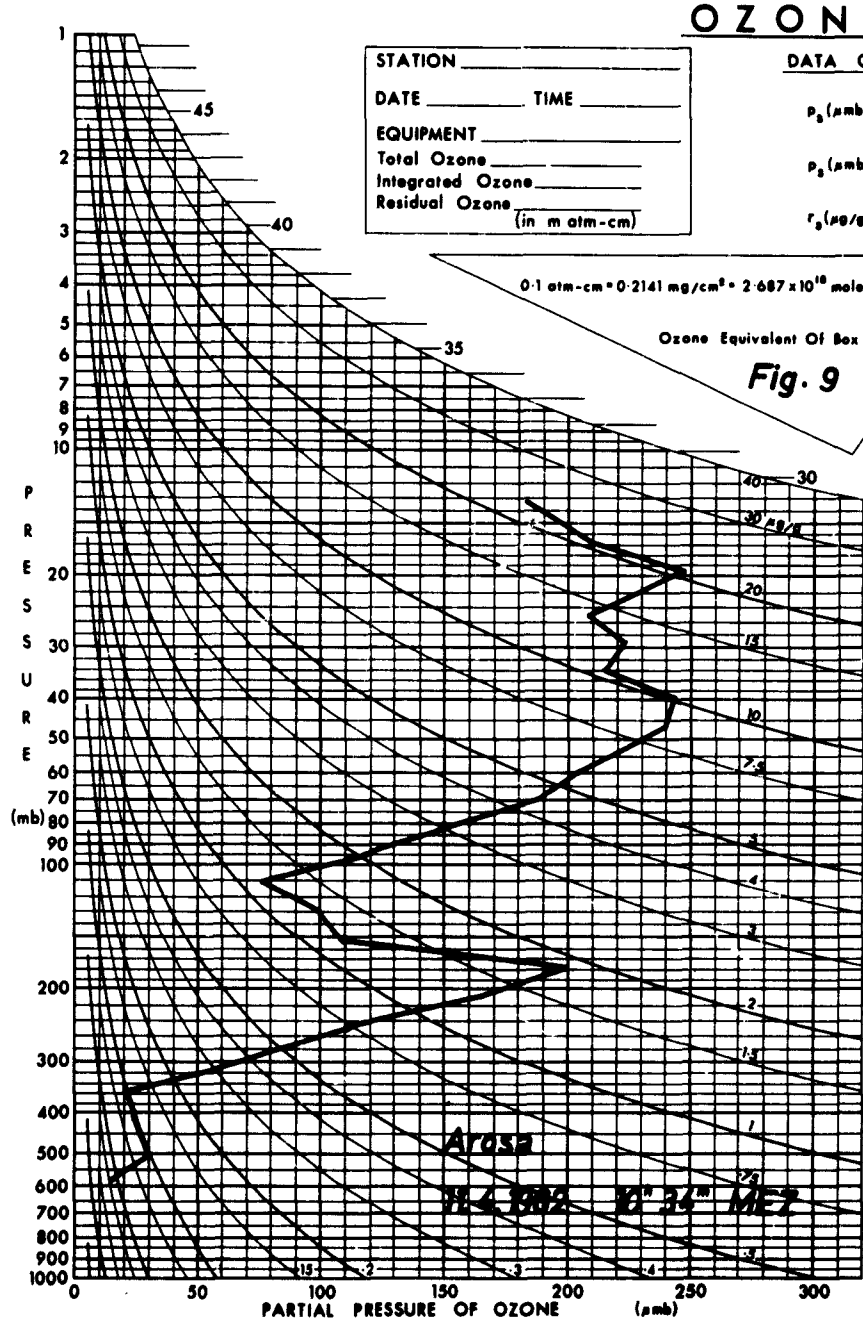

OZONAGRAM

STATION _____

DATE _____ TIME _____

EQUIPMENT _____

Total Ozone _____

Integrated Ozone _____

Residual Ozone _____ (in m atm-cm)

DATA CONVERSION EQUATIONS

$$p_s(\mu mb) = \frac{1{\cdot}732\,T\,(^\circ K)\,\rho_s(\mu g/m^3)}{1000}$$

$$p_s(\mu mb) = \frac{0{\cdot}55\,\Delta\Omega\,(m\ atm\text{-}cm)}{\Delta(\log_{10} p)}$$

$$r_s(\mu g/g) = \frac{1{\cdot}657\,p_s(\mu mb)}{p(mb)}$$

0·1 atm-cm = 0·2141 mg/cm² = 2·687 x 10¹⁸ molecules/cm² =

Ozone Equivalent Of Box Area

Fig. 10

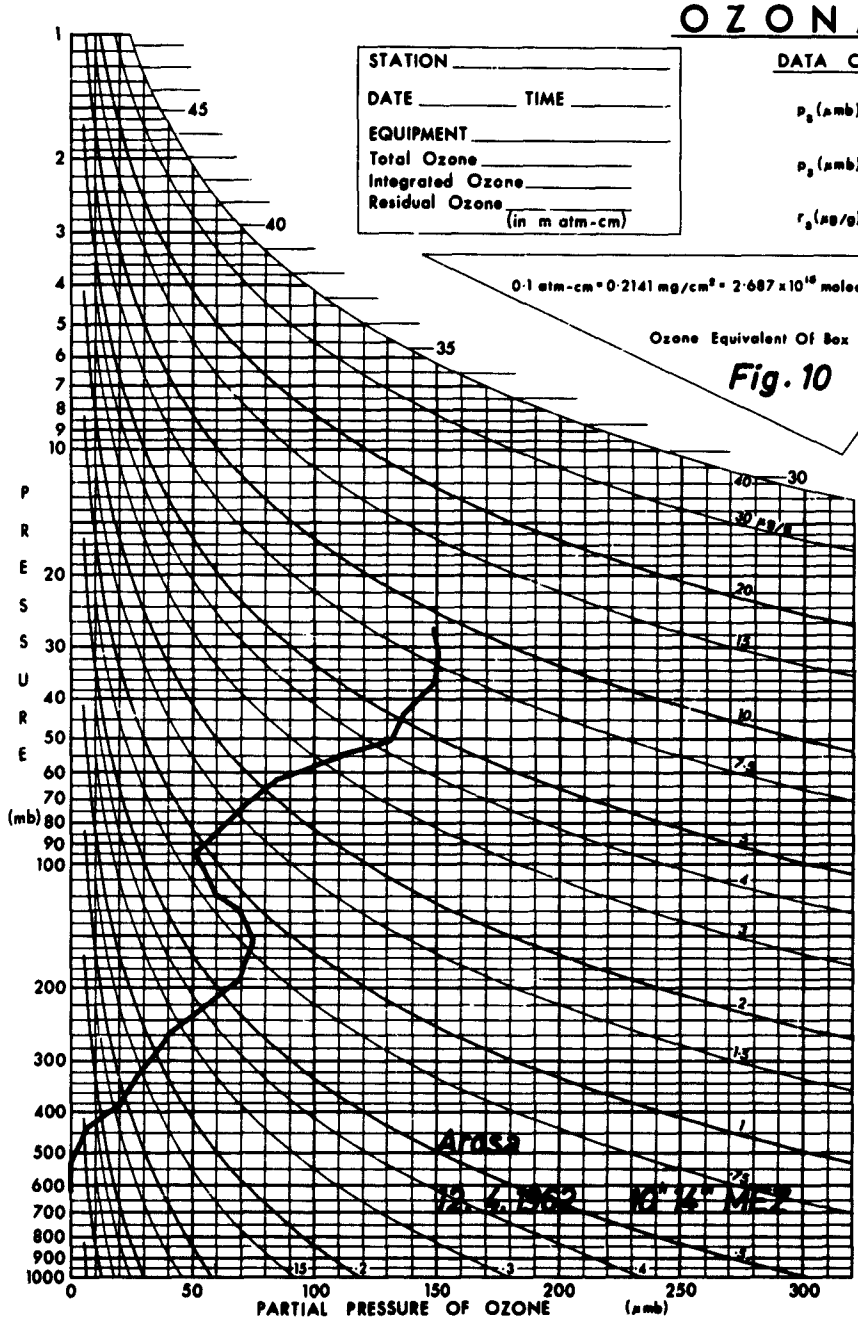

OZONAGRAM

STATION _____

DATE _____ TIME _____

EQUIPMENT _____

Total Ozone _____

Integrated Ozone _____

Residual Ozone _____ (in m atm-cm)

DATA CONVERSION EQUATIONS

$$p_3(\mu mb) = \frac{1{\cdot}732\,T\,(^\circ K)\,\rho_3(\mu g/m^3)}{1000}$$

$$p_3(\mu mb) = \frac{0{\cdot}55\,\Delta\Omega\,(m\ atm\text{-}cm)}{\Delta(\log_{10} p)}$$

$$r_3(\mu g/g) = \frac{1{\cdot}657\,p_3(\mu mb)}{p(mb)}$$

0·1 atm-cm = 0·2141 mg/cm² = 2·687 × 10¹⁸ molecules/cm² =

Ozone Equivalent Of Box Area

Fig. 11

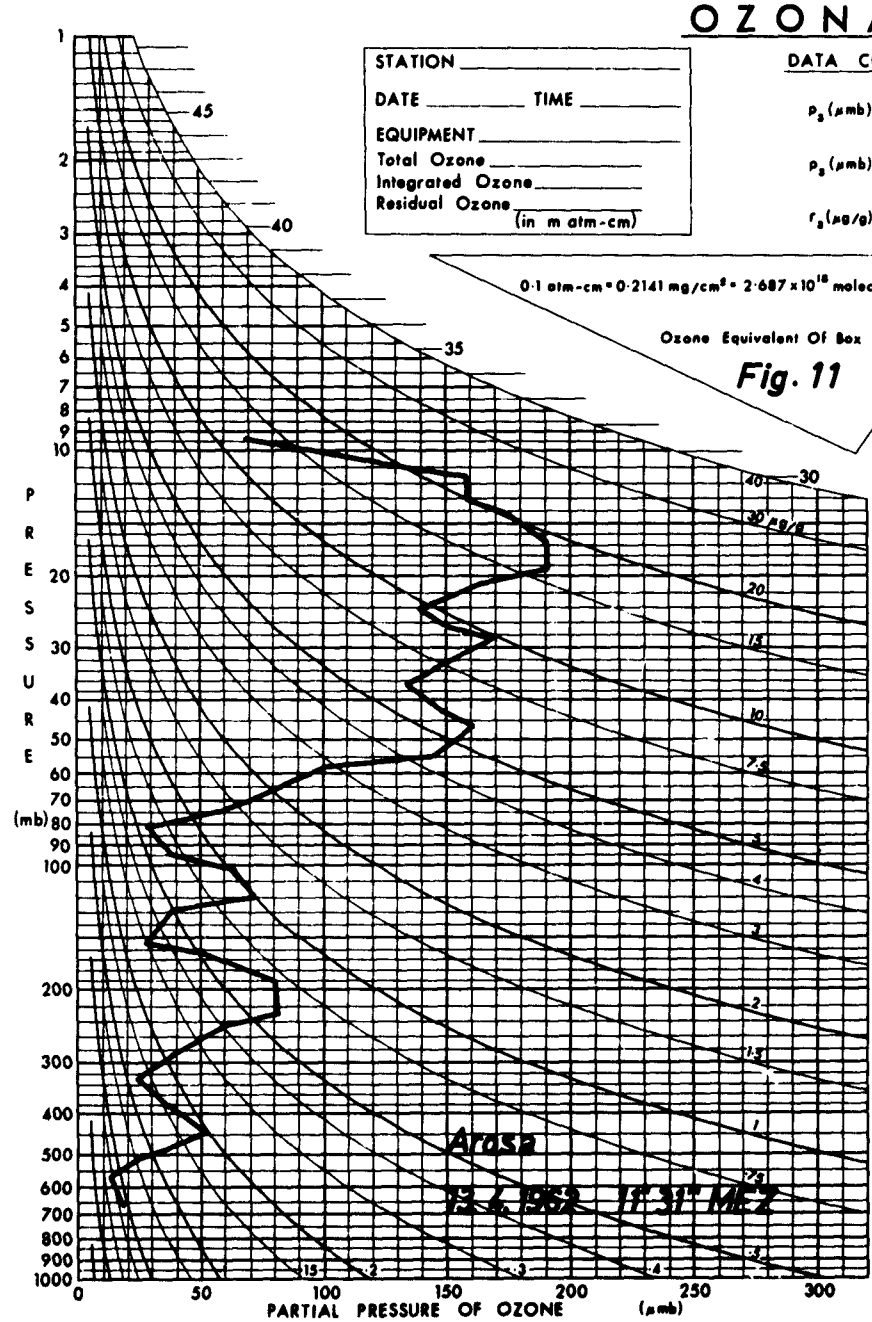

OZONAGRAM

STATION _____

DATE _____ TIME _____

EQUIPMENT _____

Total Ozone _____

Integrated Ozone _____

Residual Ozone _____ (in m atm-cm)

DATA CONVERSION EQUATIONS

$$p_s(\mu mb) = \frac{1{\cdot}732\,T\,(^\circ K)\,\rho_s(\mu g/m^3)}{1000}$$

$$p_s(\mu mb) = \frac{0{\cdot}55\,\Delta\Omega\,(m\ atm\text{-}cm)}{\Delta(\log_{10} p)}$$

$$r_s(\mu g/g) = \frac{1{\cdot}657\,p_s(\mu mb)}{p(mb)}$$

0·1 atm-cm = 0·2141 mg/cm² = 2·687 x 10¹⁸ molecules/cm² =

Ozone Equivalent Of Box Area

Fig. 12

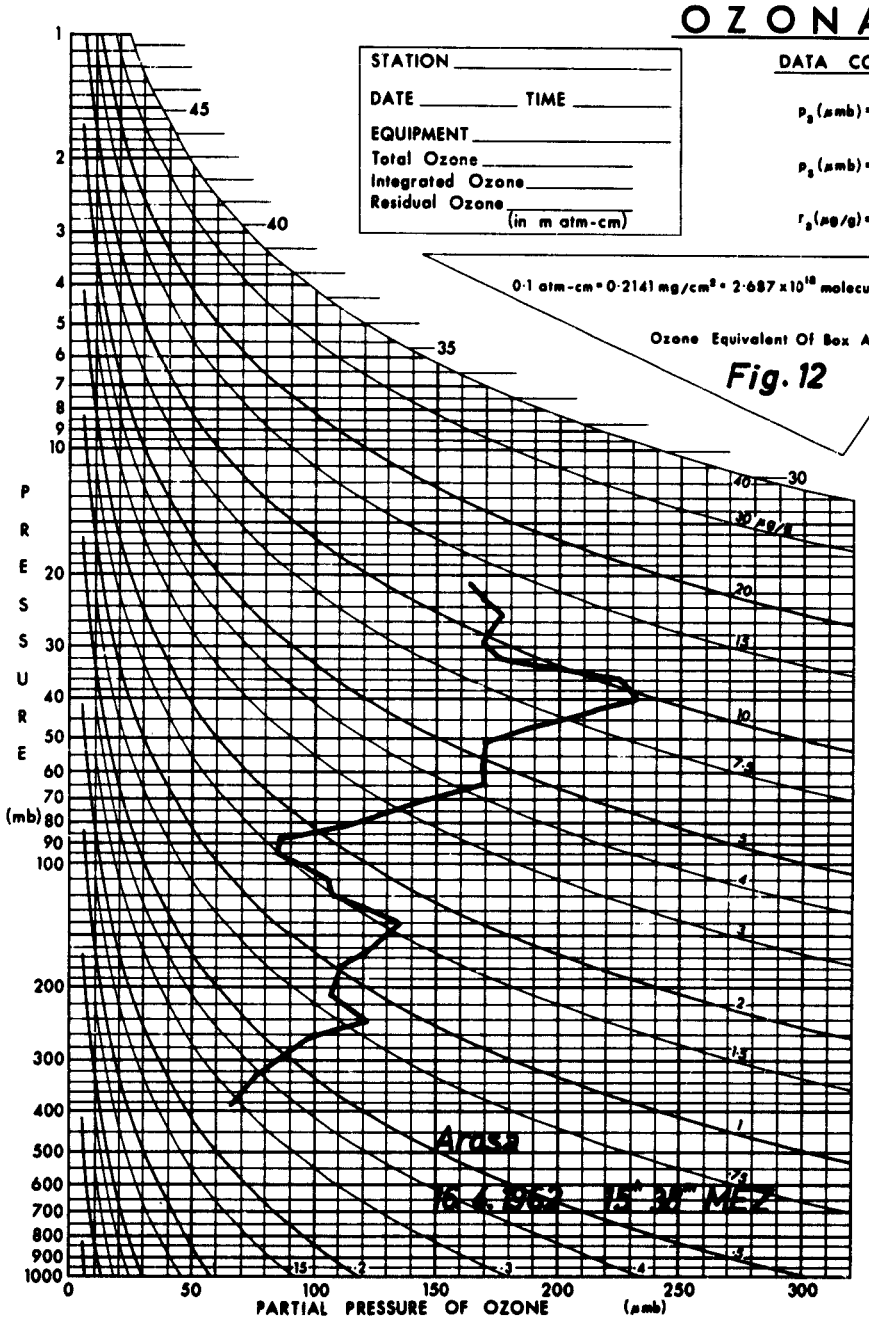

OZONAGRAM

STATION _____

DATE _____ TIME _____

EQUIPMENT _____

Total Ozone _____

Integrated Ozone _____

Residual Ozone _____ (in m atm-cm)

DATA CONVERSION EQUATIONS

$$p_s(\mu mb) = \frac{1{\cdot}732\,T\,(^\circ K)\,\rho_s(\mu g/m^3)}{1000}$$

$$p_s(\mu mb) = \frac{0{\cdot}55\,\Delta\Omega\,(m\ atm\text{-}cm)}{\Delta(\log_{10} p)}$$

$$r_s(\mu g/g) = \frac{1{\cdot}657\,p_s(\mu mb)}{p(mb)}$$

0·1 atm-cm = 0·2141 mg/cm² = 2·687 x 10^{18} molecules/cm² = Ozone Equivalent Of Box Area

Fig.13

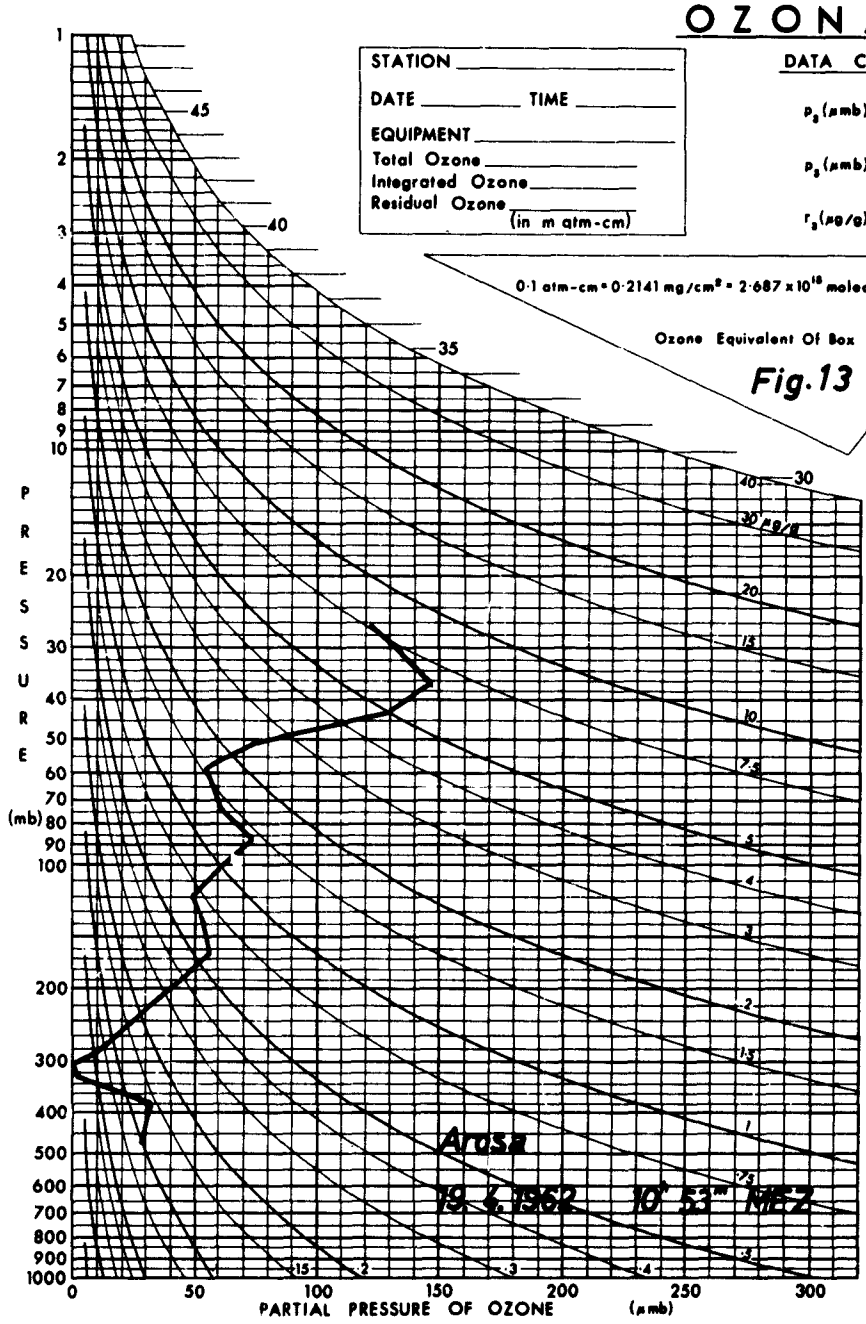

1962

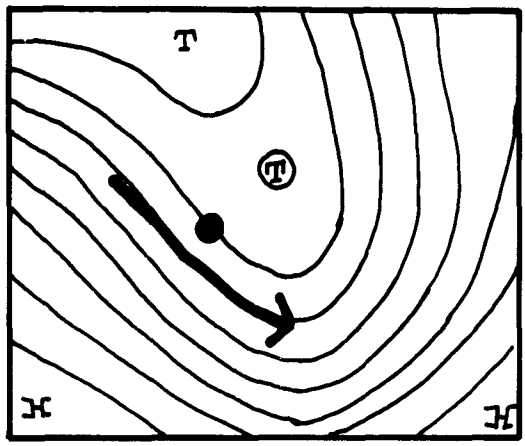

7.4.

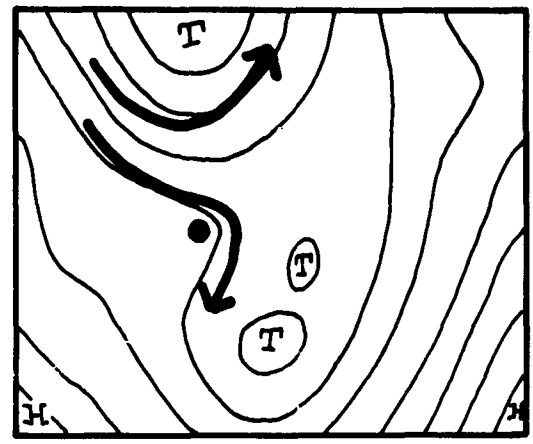

13.4.

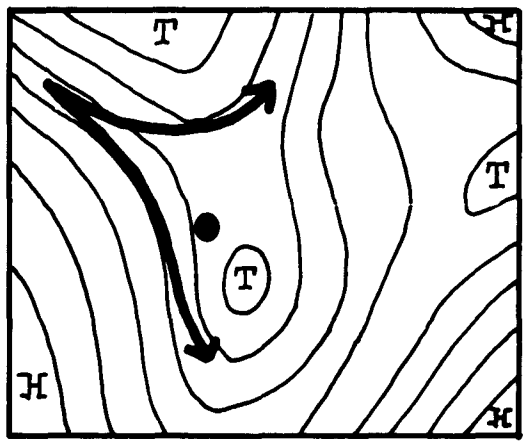

11.4.

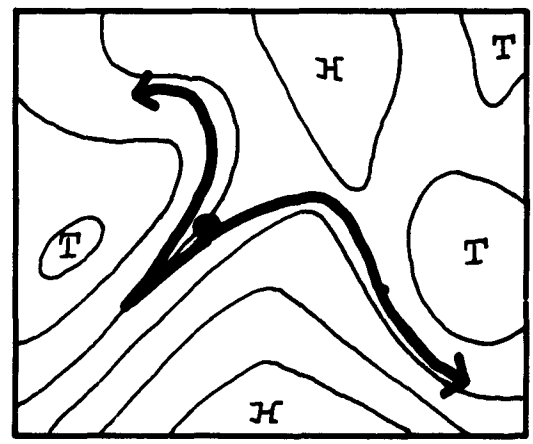

16.4.

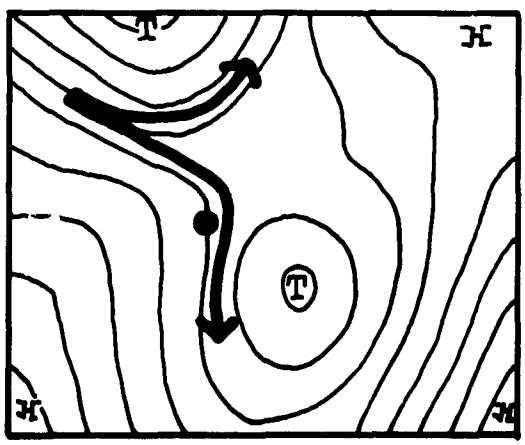

12.4.

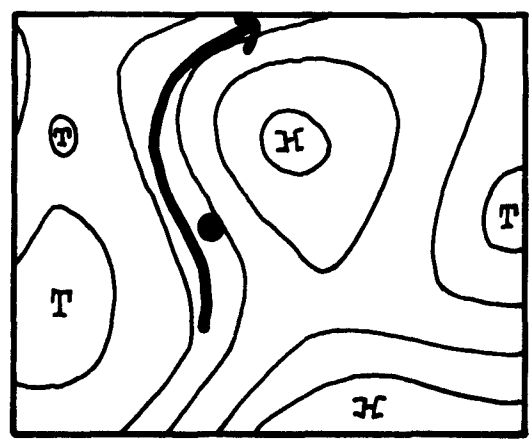

19.4.

Fig. 14

Fig. 15

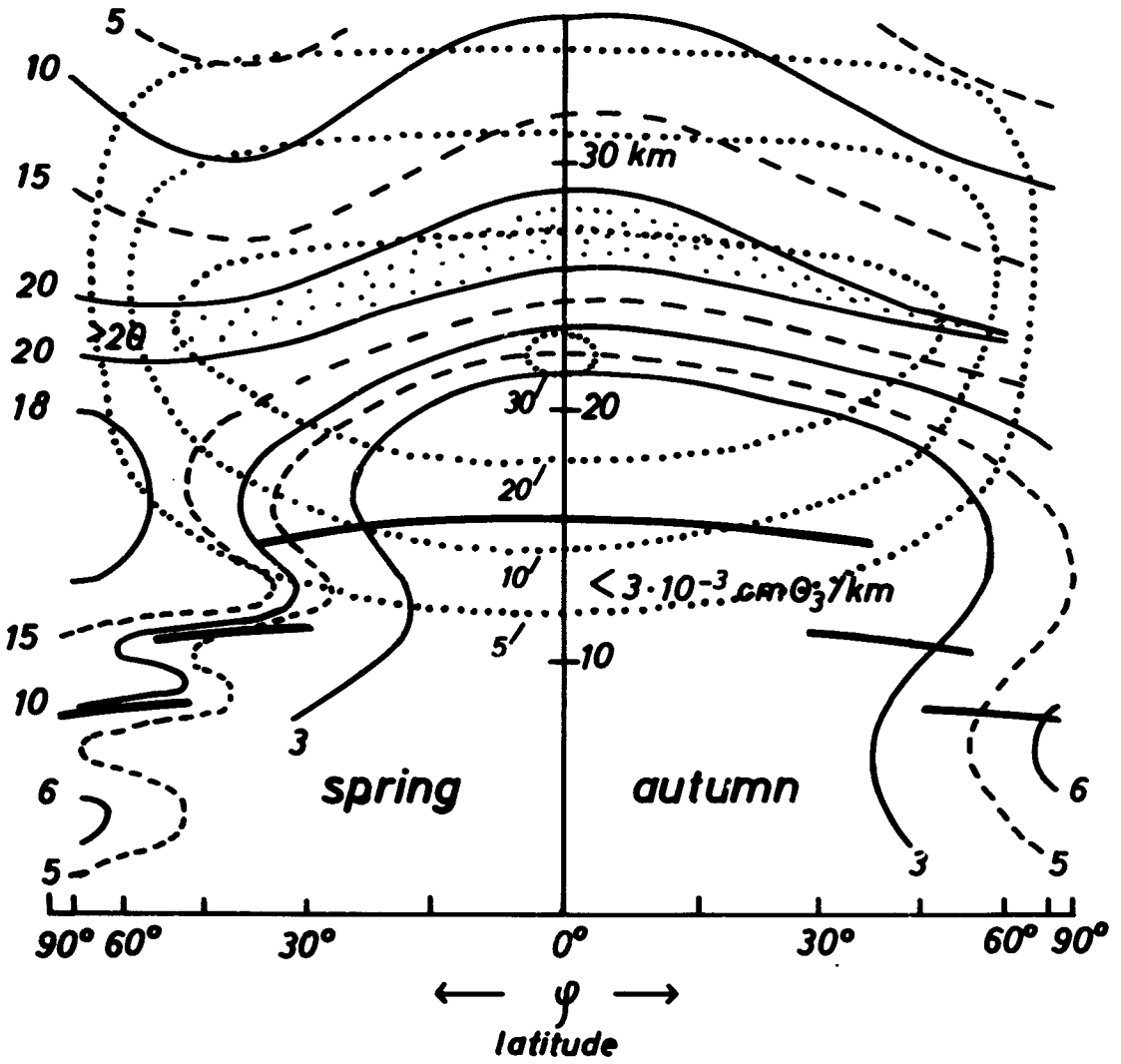
5
10
15
20
20
18
15
10
6
5
>28
30 km
30
20
20
10
5
10
3
spring
autumn
3
6
5
$< 3 \cdot 10^{-3}$ cm O_3/km
90° 60° 30° 0° 30° 60° 90°
φ
latitude

OZONAGRAM

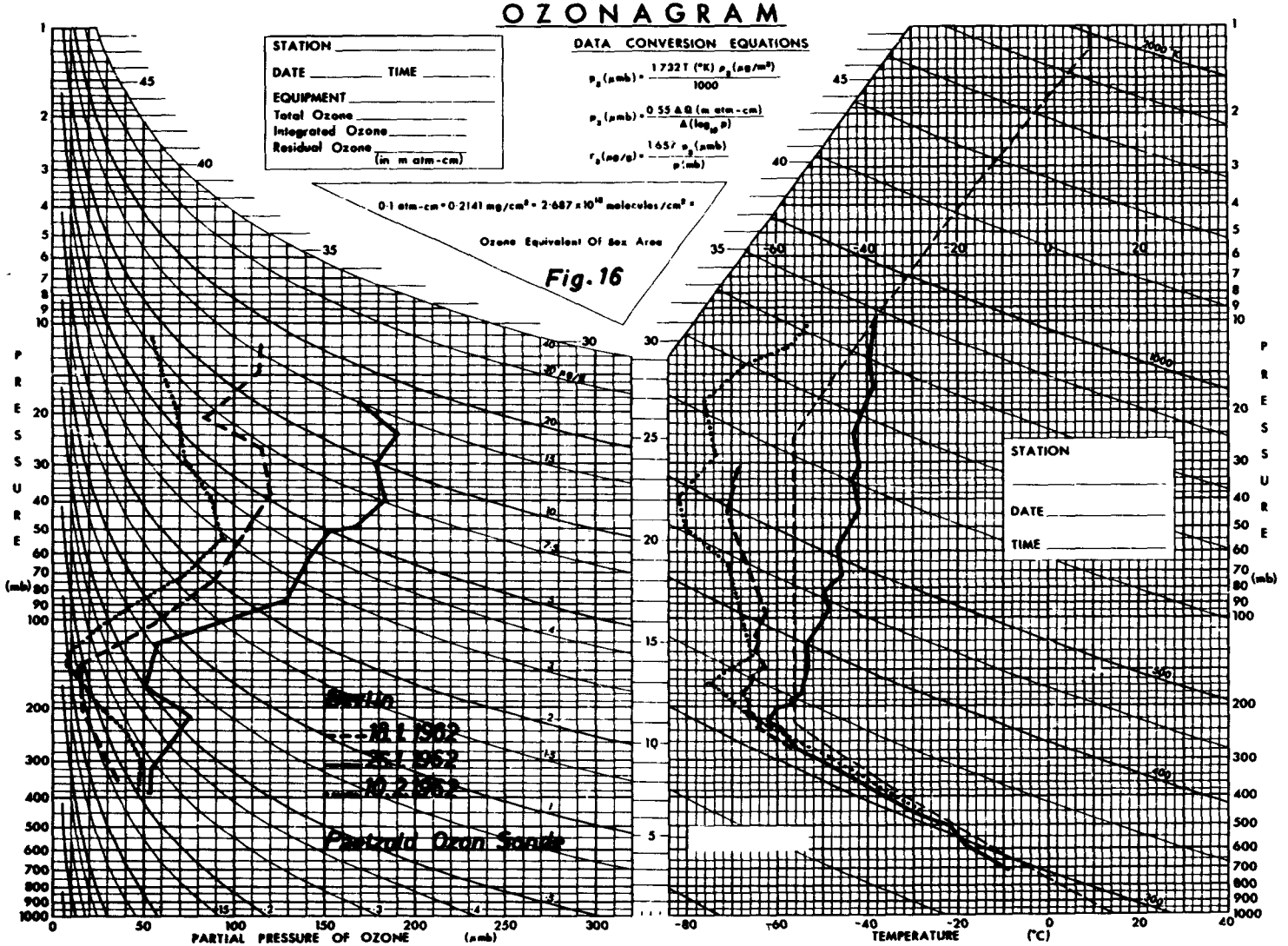
STATION
DATE TIME
EQUIPMENT
Total Ozone
Integrated Ozone
Residual Ozone
(in m atm-cm)
DATA CONVERSION EQUATIONS
0·1 atm-cm = 0·2141 mg/cm² = 2·687 x 10¹⁸ molecules/cm² =
Ozone Equivalent Of 8ex Area
Fig. 16
STATION
DATE
TIME
PRESSURE (mb)
PARTIAL PRESSURE OF OZONE (μmb)
TEMPERATURE (°C)

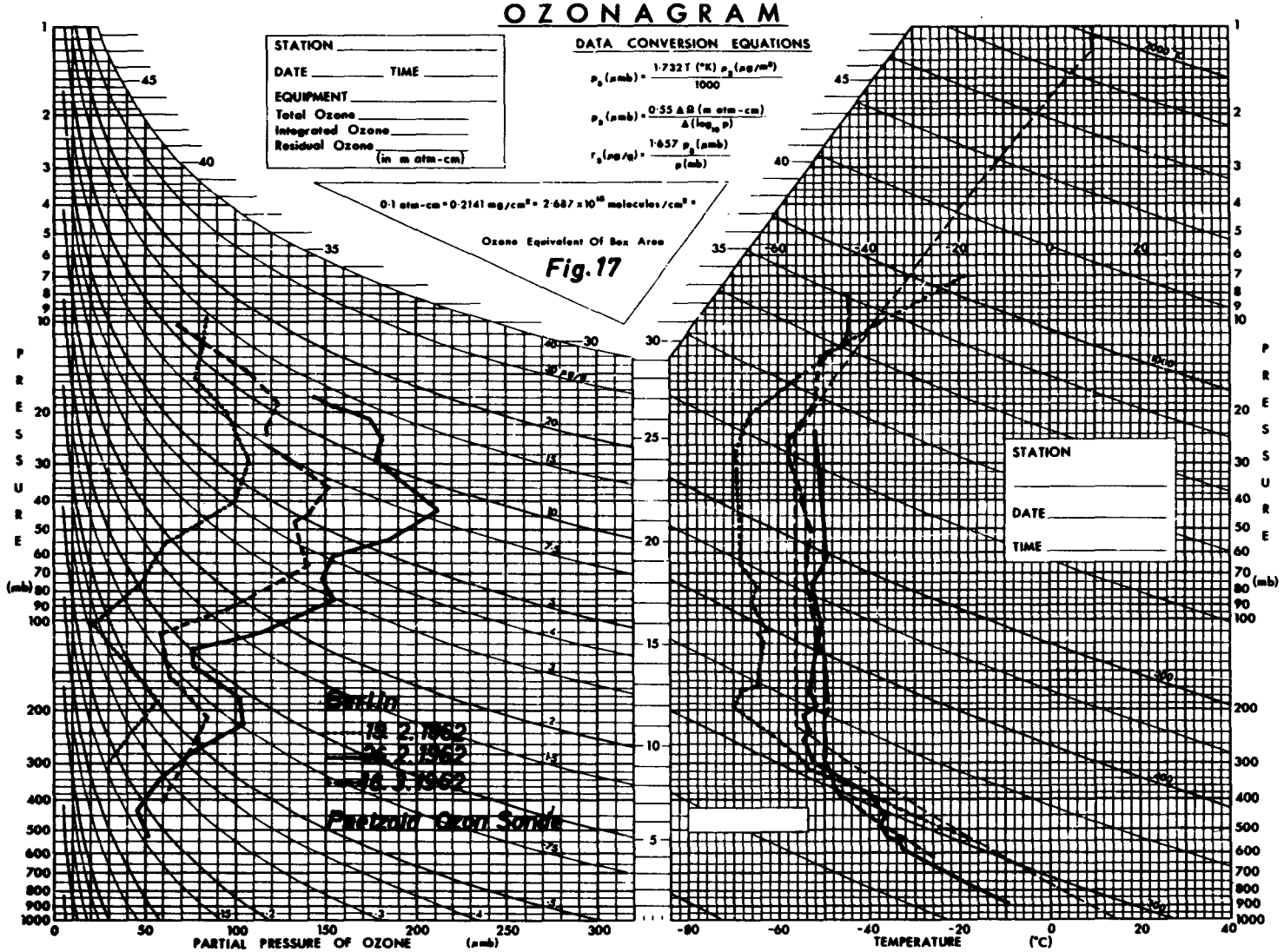
OZONAGRAM
STATION
DATE TIME
EQUIPMENT
Total Ozone
Integrated Ozone
Residual Ozone
(in m atm-cm)
DATA CONVERSION EQUATIONS
0·1 atm-cm = 0·2141 mg/cm² = 2·687 x 10¹⁸ molecules/cm² =
Ozone Equivalent Of Box Area
Fig.17
STATION
DATE
TIME
Berlin
18.2.1962
24.2.1962
26.3.1962
Pretzold Ozon Sonde
PRESSURE (mb)
PARTIAL PRESSURE OF OZONE (μmb)
TEMPERATURE (°C)

University Cologne — Contract:
Institute of Geophysics — AF 61(052)-330
T(F)R

Monitoring Agency: ARDC — Field: Geophysics

RESEARCH ON SYNOPTICAL MEASUREMENTS OF THE VERTICAL OZONE DISTRIBUTION

By H. K. Paetzold — 1 January 1963

ABSTRACT: Large scale and small scale measurements of the vertical ozone profiles and its correlation to latitude, season and weather.

USAF, European Office, ARDC, Brussels, Belgium.

University Cologne — Contract:
Institute of Geophysics — AF 61(052)-330
T(F)R

Monitoring Agency: ARDC — Field: Geophysics

RESEARCH ON SYNOPTICAL MEASUREMENTS OF THE VERTICAL OZONE DISTRIBUTION

By H. K. Paetzold — 1 January 1963

ABSTRACT: Large scale and small scale measurements of the vertical ozone profiles and its correlation to latitude, season and weather.

USAF, European Office, ARDC, Brussels, Belgium

University Cologne — Contract:
Institute of Geophysics — AF 61(052)-330
T(F)R

Monitoring Agency: ARDC — Field: Geophysics

RESEARCH ON SYNOPTICAL MEASUREMENTS OF THE VERTICAL OZONE DISTRIBUTION

By H. K. Paetzold — 1 January 1963

ABSTRACT: Large scale and small scale measurements of the vertical ozone profiles and its correlation to latitude, season and weather.

USAF, European Office, ARDC, Brussels, Belgium

University Cologne — Contract:
Institute of Geophysics — AF 61(052)-330
T(F)R

Monitoring Agency: ARDC — Field: Geophysics

RESEARCH ON SYNOPTICAL MEASUREMENTS OF THE VERTICAL OZONE DISTRIBUTION

By H. K. Paetzold — 1 January 1963

ABSTRACT: Large scale and small scale measurements of the vertical ozone profiles and its correlation to latitude, season and weather.

USAF, European Office, ARDC, Brussels, Belgium